A unified distance measurement for orientation coding in palmprint verification

Zhenhua Guo [a], Wangmeng Zuo [b], Lei Zhang [a], David Zhang [a,*]

[a] Biometrics Research Centre, The Hong Kong Polytechnic University, Hong Kong
[b] School of Computer Science and Technology, Harbin Institute of Technology, China

ABSTRACT

Orientation coding based palmprint verification methods, such as competitive code, palmprint orientation code and robust line orientation code, are state-of-the-art verification algorithms with fast matching speeds. Orientation code makes use of two types of distance measure, SUM_XOR (angular distance) and OR_XOR (Hamming distance), yet little is known about the similarities and differences between these two distance measures. In this paper, we propose a unified distance measure, of which both SUM_XOR and OR_XOR can be regarded as special cases, and provide some principles for determining the parameters of the unified distance. Experimental results show that, using the same feature extraction and coding methods, the unified distance measure gets lower equal error rates than the original distance measures.

© 2009 Elsevier B.V. All rights reserved.

1. Introduction

Nowadays, traditional token or key based personal authentication cannot meet the requirements of current applications, especially the high secure orientated ones. Automatic authentication using biometric characteristics as the substitution or complement technology is becoming more and more popular. Biometrics [1] is a study of methods for uniquely recognizing individuals based on one or more intrinsic physical or behavioral traits, including the extensively studied fingerprint [31], facial features [30], iris [29], speech, hand geometry, and palmprint [3,4]. Among these traits, fingerprint has the longest history; however, around 2% of the population could not provide clear fingerprint images [2]. Iris is another reliable trait, but its acquisition device is relatively expensive and it is not very convenient to collect. Other features, such as the face, voice, and hand geometry are not yet sufficiently accurate.

Compared with other biometric characteristics, palmprint has advantages such as high accuracy and user friendliness. During the past decades, five different classes of extraction algorithms are typically applied in palmprint recognition, subspace learning [6–12,24], multiple feature fusion [17,18], texture-based coding [5,19–22], line-like feature extraction [13–16], and wavelet analysis [25,26]. Although subspace learning [34–36] may achieve good performance on some biometric systems such as face recognition and gait recognition, they cannot effectively extract the specific features, such as the line and orientation features, existed in palmprint images, and they often require enough training samples. Multiple features [17,18] could improve the accuracy but the cost of timing and storage will be much increased. The methods in [13–16] could extract dominant line feature but may lose some fine structural information of palmprint [5], and line detection in palmprint is not an easy issue to be addressed. The wavelet coefficients could represent discriminant information of palmprint [25,26], but the feature extraction and comparison is too slow for some applications. The extraction of line-like texture feature is a particularly popular approach [19–21], in part because a palmprint contains many lines as shown in Fig. 1, including principal lines, wrinkles, and creases [5] and in part because the visual comparison of palmprint images is simple and convenient. The common tasks in line-like texture-based coding algorithms are to extract palm line orientation and compare similarity between different images. The ideal is to produce an orientation code that is accurate and has a fast matching speed, or in other words, a short feature extraction time.

One recently proposed class of methods that have achieved high speeds and accuracies [19–21] code line orientation information by viewing palm lines as negative lines. One such method is which applied six real parts of Gabor filters to the

* Corresponding author.
   E-mail addresses: cszguo@comp.polyu.edu.hk (Z. Guo), cswmzuo@gmail.com (W. Zuo), cslzhang@comp.polyu.edu.hk (L. Zhang), csdzhang@comp.polyu.edu.hk (D. Zhang).
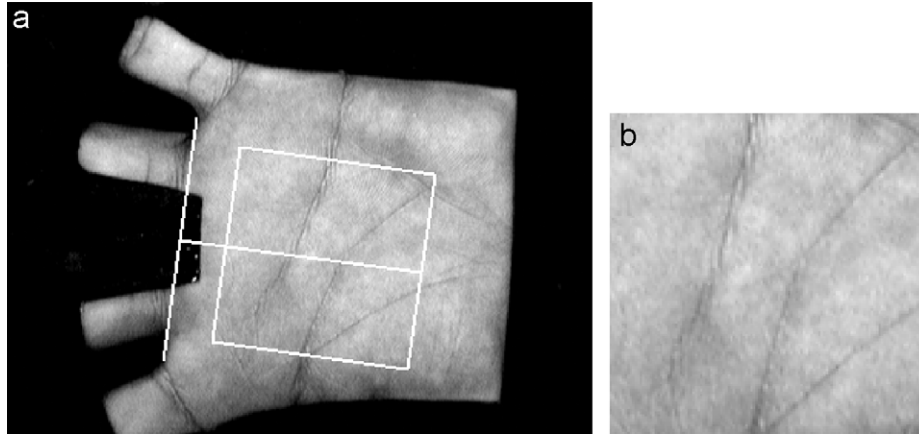
Fig. 1. (a) A sample palmprint image [28] and (b) its region of interest (ROI).

image and selected one orientation for each local region. The extracted feature was called the competitive code (CompCode) and the dissimilarity between two features is measured using the angular distance (SUM_XOR distance) [19]. Wu et al. [20] used a similar idea but used four self-devised directional templates to shorten the feature extraction time. In that case the extracted code was called palmprint orientation code (POC) and the distance was computed using the Hamming distance (OR_XOR distance). Jia et al. [21] proposed to extract orientation information using modified finite Radon transform (MFRAT). The extracted feature was called robust line orientation code (RLOC) and again the distance measure was the Hamming distance.

All of these state-of-the-art algorithms apply a common approach for feature extraction: several filters or masks with different orientations are convolved with the image, and then a criterion is applied to determine the "dominant" orientation. While both approaches to match the orientation code have been shown to be fast, and in [23], Kong claimed that the angular distance is superior to the Hamming distance but without any experimental support, little work has been done to date to compare the two distance measures. And even if it does turn out that angular distance has higher verification accuracy than the Hamming distance, it is possible that these two distance measures are complementary and the combination of them would outperform either one of them.

In this paper, we propose a unified distance measure and then show that the angular and the Hamming distance measures (SUM_XOR and OR_XOR) can be regarded as the special cases of the proposed measure. We also discuss principles for determining the parameters of the unified distance and present experimental results show that the same feature extraction and coding methods using the unified distance measure can achieve lower equal error rates (EER) than the original distance measures.

The rest of paper is organized as follows. In Section 2 we present a survey of current research on three orientation coding based feature extraction methods and their distance measures (dissimilarity distances). In Section 3 we propose a unified distance measure. Section 4 presents our experiments and results. Section 5 offers our Conclusion.

2. Review on orientation coding based palmprint verification algorithms

Fig. 2 shows an overview of the process of applying an orientation coding-based palmprint verification algorithm. The three main issues are filter design, coding of filtering responses,
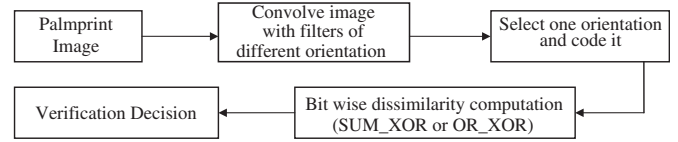

Fig. 2. Major framework of orientation coding-based palmprint verification algorithm.

and the distance measure. In the following subsections, we review three orientation coding-based algorithms, CompCode, POC and RLOC with respect to each of these issues.

2.1. Filter design

The extraction of features from a palmprint image, in particular information about the orientation of palm lines, usually involves the application of a group of filters with different orientations. Different orientation coding-based palmprint verification approaches have used different filters. CompCode [19] has used the Gabor filter, POC [20] has used directional templates, and RLOC [21] has used MRFAT.

In CompCode, the real parts of six neurophysiology-based Gabor filters with different orientations, $\theta_k = k\pi/6$ ($k=\{0, 1, 2, 3, 4, 5\}$) are used to extract the orientation information from images. The Gabor function is usually defined in the following way:

$$\psi(x,y,\omega,\theta) = \frac{\omega}{\sqrt{2\pi}\kappa} e^{-(\omega^2/8\kappa^2)(4x'^2+y'^2)}(e^{i\omega x'} - e^{-\kappa^2/2}) \qquad (1)$$

where $x' = (x-x_0)\cos\theta + (y-y_0)\sin\theta$, $y' = -(x-x_0)\sin\theta + (y-y_0)\cos\theta$, (x_0, y_0) is the center of the function; ω is the radial frequency in radians per unit length and θ is the orientation of the Gabor functions in radians. The κ is defined by $\kappa = \sqrt{2\ln 2}((2^\delta+1)/(2^\delta-1))$, where δ is the half-amplitude bandwidth of the frequency response.

To speed up the feature extraction process, POC applies a small directional template. The $0°$-directional template is defines as follows:

$$\mathbf{T}_0 = \begin{bmatrix} 1 & 1 & 1 & 1 & 1 & 1 & 1 & 1 & 1 \\ 2 & 2 & 2 & 2 & 2 & 2 & 2 & 2 & 2 \\ 3 & 3 & 3 & 3 & 3 & 3 & 3 & 3 & 3 \\ 2 & 2 & 2 & 2 & 2 & 2 & 2 & 2 & 2 \\ 1 & 1 & 1 & 1 & 1 & 1 & 1 & 1 & 1 \end{bmatrix} \qquad (2)$$

and the θ-directional template (T_θ) is obtained by rotating T_0 with an angle θ. To make the experiments be consistent, in the following we use six directional templates $\theta_k = k\pi/6$ ($k=\{0, 1, 2, 3,$

4, 5}) instead of four directional templates (0, $\pi/4$, $\pi/2$, $3\pi/4$) as proposed in [20].

To avoid "wrap around", the MRFAT proposed in RLOC uses the Radon transform. Denoting $Z_p = \{0, 1, \ldots, p-1\}$, where p is a positive integer, the MFRAT of real function $f(x, y)$ on the finite grid Z_p^2 is defined as

$$r(L_\theta) = MFRAT_f(\theta) = \sum_{(i,j) \in L_\theta} f(i, j) \qquad (3)$$

where L_θ denotes the set of points that make up a line on the lattice Z_p^2, i.e.

$$L_\theta = \{(i, j) : j = k(i - i_0), i \in Z_p\} \qquad (4)$$

where (i_0, j_0) denotes the central point of the lattice Z_p^2, and θ means the corresponding slope of L_k. Here $\theta_k = k\pi/6$ ($k = \{0, 1, 2, 3, 4, 5\}$).

2.2. Coding of orientation feature

The dominant orientation at position (x, y) is determined using the rules $\operatorname{argmin}_{\theta_k}(I(x, y) * \psi_R(x, y, \omega, \theta_k))$ (for CompCode), $\operatorname{argmin}_{\theta_k}(I(x, y) * T_{\theta_k})$ (for POC), and $\operatorname{argmin}_{\theta_k}(r(L_{\theta_k}))$ (for RLOC), where I is the input image. In CompCode, Kong et al. encoded the dominant orientation $\{0, \pi/6, \pi/3, \pi/2, 2\pi/3, 5\pi/6\}$ using three bits $\{000, 001, 011, 111, 110, 100\}$ for efficient palmprint representation and matching. Fig. 3b shows an example of CompCode. Such a coding could also be used in the POC and RLOC schemes [20,21]. Fig. 3c shows an example of the coding map of POC and Fig. 3d that of RLOC.

2.3. Distance measure

Orientation code matches using two kinds of distance measure, SUM_XOR (angular distance) and OR_XOR (Hamming distance). In CompCode [19], the angular distance between two features is defined as

$$D_{SUM\_XOR}(P, Q) = \frac{\sum_{y=1}^{M} \sum_{x=1}^{N} \sum_{i=1}^{3} P_i^b(x, y) \otimes Q_i^b(x, y)}{3 * M * N} \qquad (5)$$

where P and Q are two CompCode features. P_i^b or Q_i^b is the ith bit plane of P or Q and $\otimes$ is bitwise exclusive OR (XOR). For each pixel, the angular distance is the sum of the three XOR results on each bit. Thus the angular distance can be called the SUM_XOR distance.

In [20], the distance between two POCs is defined as follows:

$$D_{Hamming}(P, Q) = \frac{H(P, Q)}{M * N} \qquad (6)$$

where $H(P, Q)$ is defined as the number of pixels at which the values of P and Q are different. Using the bit representation as

CompCode, the distance could be rewritten as

$$D_{OR\_XOR}(P, Q) =$$
$$\frac{\sum_{y=1}^{M} \sum_{x=1}^{N} (P_0^b(x, y) \otimes Q_0^b(x, y)) | (P_1^b(x, y) \otimes Q_1^b(x, y)) | (P_2^b(x, y) \otimes Q_2^b(x, y))}{M * N} \qquad (7)$$

For each pixel, the distance defined in Eq. (7) actually performs the OR operation on the three XOR results on each bit. It is called the OR_XOR distance. RLOR uses a similar distance measure [21].

3. A unified distance measurement

In the past, research on how to represent palmprint features has attracted a lot of attention, and some work have been done on investigating the relationship between different feature extraction algorithms [22]. In contrast, little such work has been done on the distance measures. SUM_XOR and OR_XOR have been widely adopted for fast matching of orientation codes, while little comparative study has been made to investigate the difference and relations between them. In [23], Kong claimed that SUM_XOR is superior to OR_XOR but without any experimental evidence. Even SUM_XOR could achieve higher verification accuracy, it is still possible that OR_XOR and SUM_XOR would be complementary and hence the combination of them would outperform any one of them.

In this section, we propose a unified distance measure and then show that OR_XOR and SUM_XOR can be regarded as two special cases of the unified distance measure. We then discuss the principles for determining the parameters of the unified distance and compare the computational complexity of OR_XOR, SUM_XOR, and the unified distance measure.

3.1. Relation between SUM_XOR and OR_XOR

Suppose $P(x, y)$ and $Q(x, y)$ are two three-bit features extracted from the same location of two images. Using the SUM_XOR distance, there are four possible results when we compare $P(x, y)$ with $Q(x, y)$: zero-, one-, two- or three-bit difference. Denote by **a**, **b**, **c**, and **d** the numbers of pixels where the zero-, one-, two- and three-bit differences occur, respectively. We define the unified distance between P and Q

$$D_U(P, Q) = \frac{(1+K) * b + (2+K) * c + (3+K) * d}{(3+K)(a+b+c+d)} \qquad (8)$$

where K is a parameter of the unified distance measure.

It can be shown that OR_XOR and SUM_XOR are two special cases of the proposed unified distance measure. The SUM_XOR distance (angular distance) defined in Eq. (5) could be written as

$$D_{SUM\_XOR}(P, Q) = \frac{b + 2c + 3d}{3(a+b+c+d)} \qquad (9)$$
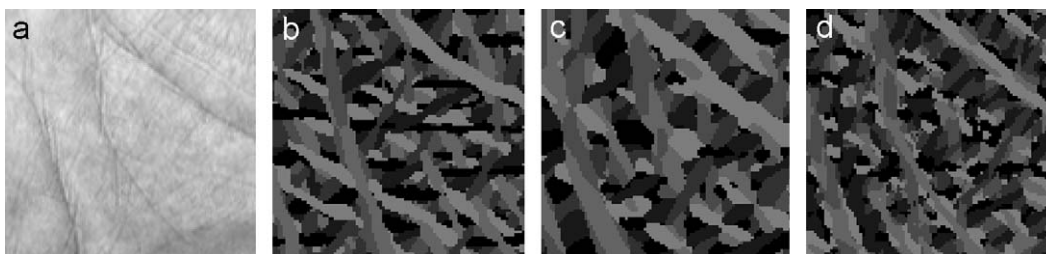

Fig. 3. One palmprint image (a) and with its three different feature maps (b) CompCode, (c) POC, and (d) RLOC. Different orientation feature is represented by different gray values.

Clearly the SUM_XOR distance is a special case of the unified distance with $K=0$. Similarly, the OR_XOR distance defined in Eq. (7) could be written as

$$D_{OR\_XOR}(P,Q) = \frac{b+c+d}{a+b+c+d} = \lim_{K \to +\infty} D_U(P,Q) \qquad (10)$$

Thus, the OR_XOR distance can also be regarded as a special case of the unified distance with $K = +\infty$. By adjusting the K value, we can get the more appropriate weights on a, b, c, and d, and thus expect that the unified distance measure would achieve a higher verification performance.

3.2. Selection of parameter K

In this section, we discuss some principles to determine the value of parameter K based on the score level fusion theory [27]. OR_XOR and SUM_XOR can be treated as two classifiers. Given two templates P and Q, the outputs of these two classifiers are $D_{SUM\_XOR}(P,Q)$ and $D_{OR\_XOR}(P,Q)$. If we adopt the weighted sum rule to combine the classification outputs $D_{SUM\_XOR}(P,Q)$ and $D_{OR\_XOR}(P,Q)$, the fusing result would be

$$D_C(P,Q) = D_{SUM\_XOR}(P,Q) + wD_{OR\_XOR}(P,Q) \qquad (11)$$

where $w > 0$ is the weight on OR_XOR. The fusing result can be given as

$$D_C(P,Q) = \frac{(1+3w)b+(2+3w)c+(3+3w)d}{3(a+b+c+d)} \qquad (12)$$

$$D_C(P,Q) = \frac{3+K}{3}D_U(P,Q) \quad \text{when } K = 3w \qquad (13)$$

It is obvious that the unified distance measure is proportional to the weighted sum of OR_XOR and SUM_XOR with $K = 3w$. In real application, the selection of K, like in many other score level fusion [27] technique, is not a trivial issue. It could be relied on the individual modal's accuracy [32], or be done by using a small portion of the data as training set to tune the parameter [7]. Usually, the weight is strongly related with the data set and the feature map's discrimination. For example, if OR_XOR has better result than SUM_XOR on a given data set, the optimal value of K should be bigger than 3 ($w > 1$); otherwise, it will be smaller than 3 ($w \le 1$).

3.3. Computational complexity

The proposed unified distance preserves the fast matching property and could be implemented in bit-wise operation. In this subsection, we compare the computational complexity of OR_XOR, SUM_XOR, and the unified distance measure.

Suppose P and Q are of $M*N$ pixels and there are three bits for each pixel. According to Eq. (5), SUM_XOR needs $3*M*N$ times XOR operations and $3*M*N$ times SUM operations. While OR_XOR in Eq. (7) requires the same number of XOR operations, $2*M*N$ times OR operations and $M*N$ times SUM operations. Usually, the bit-wise operation OR is much faster than integer-wise SUM operation. So OR_XOR is a little faster than SUM_XOR.

For the unified distance measures, Eq. (8) could be rewritten as

$$D_U(P,Q) = \frac{-Ka+b+2c+3d}{(3+K)a+b+c+d} + \frac{K}{3+K} = \frac{D'_U(P,Q)}{3+K} + \frac{K}{3+K} \qquad (14)$$

$$D'_U(P,Q) = \frac{-K*a+b+2c+3d}{a+b+c+d} \qquad (15)$$

Since K is a constant value, it will not influence the distance relationship. For example, if $D_U(A,B) > D_U(A,C)$, then $D'_U(A,B) > D'_U(A,C)$. So Eqs. (14) and (15) could be regarded as equivalent form for recognition.

Eq. (15) could be implemented in bit-wise operation as

$$D'_U(P,Q) = \frac{-K*a+b+2c+3d}{a+b+c+d}$$

$$= \frac{-K*\sum_{y=1}^{M}\sum_{x=1}^{N}(P_0^b(x,y)\otimes Q_0^b(x,y))|(P_1^b(x,y)\otimes Q_1^b(x,y))|(P_2^b(x,y)\otimes Q_2^b(x,y))}{M*N}$$

$$+ \frac{\sum_{y=1}^{M}\sum_{x=1}^{N}\sum_{i=1}^{3}P_i^b(x,y)\otimes Q_i^b(x,y)}{M*N} \qquad (16)$$

It needs $3*M*N$ times XOR operations, $2*M*N$ times OR operations, and $4*M*N$ times SUM operations. Though the complexity is little higher than SUM_XOR and OR_XOR, the unified distance measure is still fast enough for real time applications.

4. Experimental results

In this section, we compare the performance of two different distance measures and investigate the effect of K on Eq. (15) using two public palmprint databases and three feature extraction methods.

4.1. Experiment results on PolyU database [28]

4.1.1. Database and test protocol
This public database contains 7752 palmprint images from 193 individuals. The database was collected in two sessions. In each session, the subject was asked to provide about 10 palmprint images each from his left and right palms. Each person provided around 40 images. The average interval between the first and the second collection was 69 days.

The palmprint verification tests matched each palmprint image against all the other palmprint images in the database. A match was counted as genuine if the two palmprint images were from the same palm. Otherwise, it was counted as an impostor. There were 30,042,876 matches with 74,068 being genuine. Due to page limitation, the EER, the point when false accept rate (FAR) is equal to false reject rate (FRR), is used to evaluate the accuracy.

The central part ($128*128$) of the palm image was cropped using a region of interest (ROI) extraction algorithm similar to that described in [5]. To reduce the influence of imperfect ROI extraction, we translate the features vertically and horizontally in a small range. A minimal distance obtained by translated matching is regarded as the final distance. The ranges of the translation are all set -4–4 in this section.

4.1.2. Verification accuracy comparison and discussion
Fig. 4 shows the EERs using different K values. Because we add some morphological operations to overcome the broken finger problem caused by shading during ROI extraction, better results were achieved than the previous publication [19–21].

As shown in Fig. 4, the EER drops to a minimal point when K is small, then it increases and gradually stabilizes. This is because OR_XOR and SUM_XOR have different properties. Fusing those increases accuracy when K is small but as K increases, the accuracy will change gradually to that of OR_XOR. Fig. 5 shows an example. Using original SUM_XOR distance, the same palm images will be wrongly classified because the distance is bigger than that of the different palm images. If we use a different K values, it will easy to distinguish the same palm images from the different palm images.

Table 1 lists part of the EERs with optimal K values. Compared with the original distance (italic number) used in each method, the optimal K value (shown in bracket) reduces the EER by up to 22% ($0.0379 \to 0.0298$), 25% ($0.2341 \to 0.1761$), and 20% ($0.0820 \to 0.0656$)

for CompCode, POC, and RLOC, respectively. There is no common optimal K value for the unified distance. As discussed in Section 3.2 this value is related to the performance of SUM_XOR and OR_XOR. For example, when EER of SUM_XOR is lower than that of OR_XOR, smaller K will get superior results. Negative K value will drop the performance significantly, and this is intuitive because bigger **a** should occur on genuine and it plays an important role for discrimination. We also found that in this database, SUM_XOR is better than OR_XOR. This finding is consistent with the claim by Kong [23], i.e. angular distance is superior to Hamming distance.

4.2. Experimental results on CASIA database [33]

4.2.1. Database and test protocol

The CASLA database contains 5239 palmprint images from 301 individuals. To the best of our knowledge, this database is the largest public available database in term of the number of
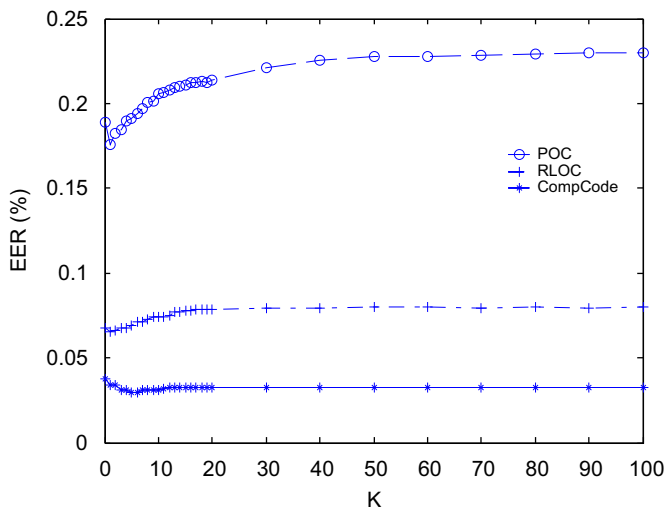
subjects. The samples were collected in one session only. The subject was asked to provide about eight palmprint images from his/her left and right palms.

The same test protocol and matching scheme stated above is used in this section. There were 13,710,466 (two poor quality images were excluded from our experiment, so the actual number of pictures is 5237) matches with 20,567 being genuine. EER is used to evaluate the accuracy.

4.2.2. Verification accuracy comparison and discussion

Fig. 6 shows the EERs using different K values and Table 2 lists part of the EERs with optimal K values. Similar to Fig. 4, the EER drops to a minimal point, and then it increases and gradually stabilizes. The optimal K value could reduce the EER compared with original distance metric. Unlike the results in PolyU database, OR_XOR gets better result than SUM_XOR for all feature extraction methods. This finding shows that it is hard to draw a conclusion that the angular distance is superior to the Hamming distance.

The accuracy of CASIA database is much lower than that of PolyU. This is mainly caused by three reasons. First, the size of the database of CASIA is much larger than PolyU, which brings difficulty for classification. Second, there are no pegs to restrict postures and positions of palms during CASIA data collection, which brings large degree of freedom. Finally, the image quality of CASIA is not as good as that of PolyU. As shown in Fig. 7, lot of detailed palmprint information is lost in CASIA database.

Fig. 4. EER vs K.

Table 1
EER under different K values and different feature extraction algorithms.

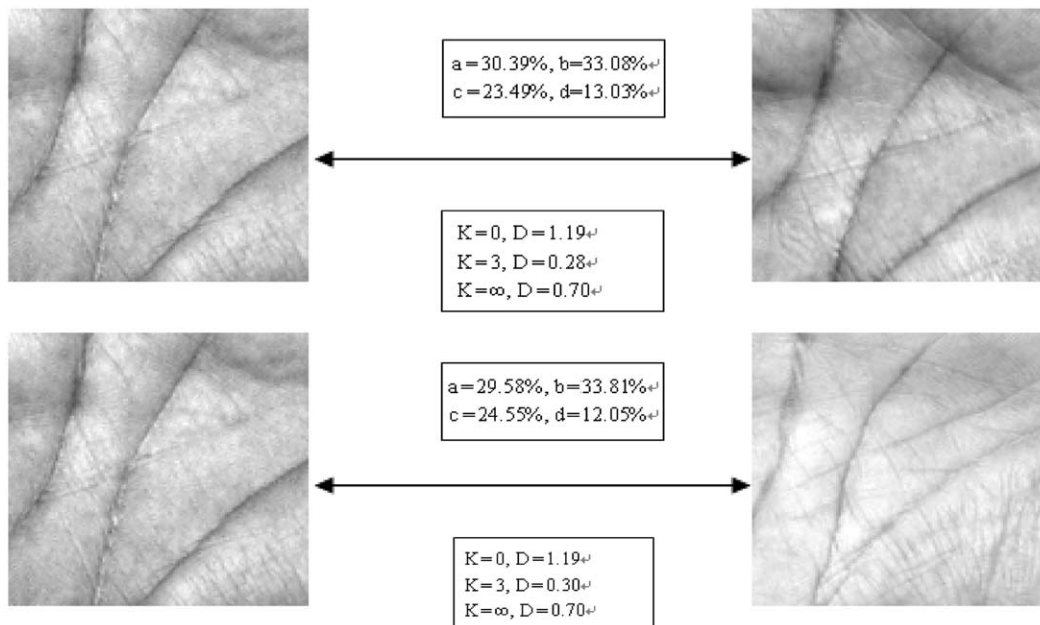| EER (%)	CompCode	POC	RLOC
0 (SUM_XOR)	*0.0379*	0.1887	0.0678
Optimal K	0.0298 (K=5)	0.1761 (K=1)	0.0656 (K=1)
+∞ (OR_XOR)	0.0325	*0.2341*	*0.0820*

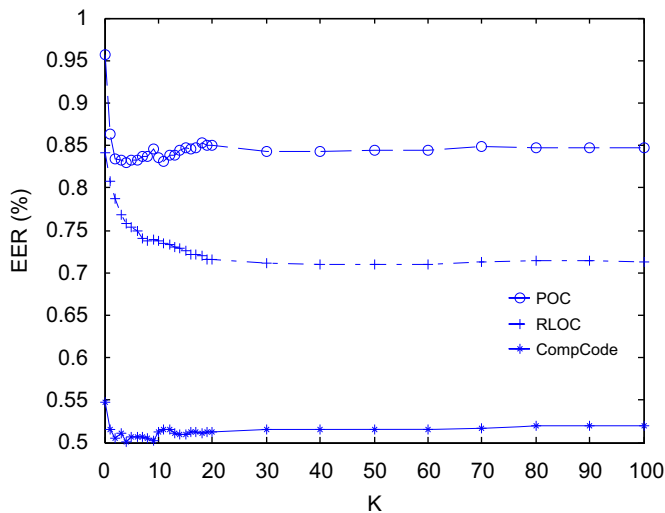**Fig. 5.** The matching results with different K values. CompCode is applied on the three images.

Fig. 6. EER vs *K*.

Table 2
EER under different *K* values and different feature extraction algorithms.

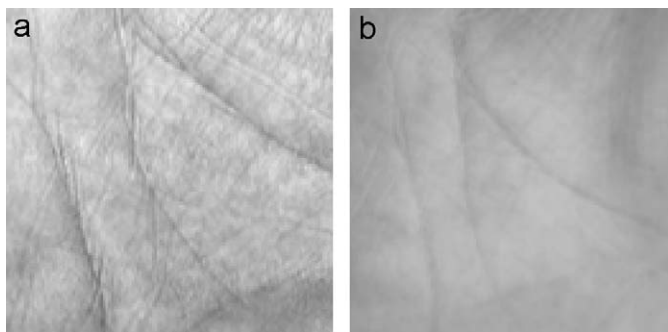| EER (%)	CompCode	POC	RLOC
0 (SUM_XOR)	*0.5475*	0.9575	0.8407
Optimal *K*	0.5006 (*K*=4)	0.8294 (*K*=4)	0.7092 (*K*=50)
+∞ (OR_XOR)	0.5190	*0.8547*	*0.7138*

Fig. 7. (a) A sample palmprint of PolyU [28] and (b) A sample palmprint of CASIA [33].

Table 3
Execution times of different distance measures.

Measure	Average time (ms)
SUM_XOR (Eq. (5))	0.058
OR_XOR (Eq. (7))	0.052
Unified distance (Eq. (15))	0.070

4.3. Matching speed

Table 3 shows the matching speed of different distance measures by average execution times. The ordinal relationship is accord with our computational complexity discussion in Section 3.3. The experiment is implemented using Visual C++6.0 on a PC with Windows XP, E6650 CPU (2.33GHz) and 4GB Ram. Although the proposed unified distance takes a little longer than OR_XOR, it could increase the accuracy and still fast enough for most of applications. For example, for a 1–10 000 identification comparison, the matching using the proposed distance takes about 0.7 s.

5. Conclusions

In this paper we discussed three state-of-the-art palmprint verification algorithms and their feature extraction and matching metrics. After analyzing the two distance metrics, we proposed a unified distance for orientation-based coding. The two widely used distance metrics are two special cases of the proposed distance. The proposed distance measure was evaluated on two large public databases. The palmprint verification results showed that the proposed unified distance achieves lower EER than the each of the two previously used distances on both databases. We also empirically found that OR_XOR is not inferior to SUM_XOR but has a faster matching speed. The proposed matching distance could also be applied to other coding based palmprint verification algorithms, such as OLOF [22].

References

[1] H.L. Lee, R.E. Gaensslen (Eds.), Advances in Fingerprint Technology, second ed., CRC Press, London, 2001.
[2] NIST Report on the United States Congress, Summary of NIST standards for biometric accuracy, temper, resistance, and interoperability, 2001.
[3] D. Zhang, Automated Biometrics—Technologies and Systems, Kluwer Academic Publishers, Dordrecht, 2000.
[4] A. Jain, R. Bolle, S. Pankanti (Eds.), Biometrics: Personal Identification in Network Society, Kluwer Academic, Boston, 1999.
[5] D. Zhang, W. Kong, J. You, M. Wong, Online palmprint identification, IEEE Transactions on Pattern Analysis and Machine Intelligence 25 (2003) 1041–1050.
[6] G. Lu, D. Zhang, K. Wang, Palmprint recognition using eigenpalms features, Pattern Recognition Letters 24 (2003) 1463–1467.
[7] S. Ribaric, I. Fratric, A biometric identification system based on eigenpalm and eigenfinger features, IEEE Transactions on Pattern Analysis and Machine Intelligence 27 (2005) 1698–1709.
[8] X. Wu, D. Zhang, K. Wang, Fisherpalm based palmprint recognition, Pattern Recognition Letters 24 (2003) 2829–2838.
[9] T. Connie, T. Andrew, K. Goh, An automated palmprint recognition system, Image and Vision Computing 23 (2005) 501–505.
[10] D. Hu, G. Feng, Z. Zhou, Two-dimensional locality preserving projections (2DLPP) with its application to palmprint recognition, Pattern Recognition 40 (2007) 339–342.
[11] J. Wang, W. Yau, A. Suwandy, E. Sung, Person recognition by fusing palmprint and palm vein images based on "Laplacianpalm" representation, Pattern Recognition 41 (2008) 1531–1544.
[12] X.-Y. Jing, Y.-F. Yao, D. Zhang, J.-Y. Yang, M. Li, Face and palmprint pixel level fusion and Kernel DCV-RBF classifier for small sample biometric recognition, Pattern Recognition 40 (2007) 3209–3224.
[13] C.-C. Han, H.-L. Cheng, C.-L. Lin, K.-C. Fan, Personal authentication using palmprint features, Pattern Recognition 36 (2003) 371–381.
[14] C.-L. Lin, T.C. Chung, K.-C. Fan, Palmprint verification using hierarchical decomposition, Pattern Recognition 38 (2005) 2639–2652.
[15] X. Wu, D. Zhang, K. Wang, Palm line extraction and matching for personal authentication, IEEE Transactions on System, Man, and Cybernetics, Part A 36 (2006) 978–987.
[16] D.-S. Huang, W. Jia, D. Zhang, Palmprint verification based on principal lines, Pattern Recognition 41 (2008) 1316–1328.
[17] A. Kumar, D. Zhang, Personal authentication using multiple palmprint representation, Pattern Recognition 38 (2005) 1695–1704.

[18] A. Kong, D. Zhang, M. Kamel, Palmprint identification using feature-level fusion, Pattern Recognition 39 (2006) 478–487.

[19] A. Kong, D. Zhang, Competitive coding scheme for palmprint verification, in: International Conference on Pattern Recognition, 2004, pp. 520–523.

[20] X. Wu, K. Wang, D. Zhang, Palmprint authentication based on orientation code matching, in: Audio- and Video-Based Biometric Person Authentication, 2005, pp. 555–562.

[21] W. Jia, D.-S. Huang, D. Zhang, Palmprint verification based on robust line orientation code, Pattern Recognition 41 (2008) 1504–1513.

[22] Z. Sun, T. Tan, Y. Wang, S.Z. Li, Ordinal palmprint representation for personal identification, in: IEEE Computer Society Conference on Computer Vision and Pattern Recognition, 2005, pp. 279–284.

[23] A. Kong, Palmprint identification based on generalization of IrisCode, Ph.D Thesis, University of Waterloo, 2007.

[24] W. Jia, D. Huang, D. Tao, D. Zhang, Palmprint identification based on directional representation, in: IEEE International Conference on Systems, Man and Cybernetics, 2008, pp. 1562–1567.

[25] L. Zhang, D. Zhang, Characterization of palmprint by wavelet signatures via directional context modeling, IEEE Transactions on System, Man, and Cybernetic, Part B 34 (2004) 1335–1347.

[26] G. Y. Chen, T. D. Bui, A. Krzyak, Palmprint classification using dual-tree complex wavelets, in: International Conference on Image Processing, 2006, pp. 2645–2648.

[27] A.A. Ross, K. Nadakumar, A.K. Jain, Handbook of Multibiometrics, Springer, Berlin, 2006.

[28] PolyU Palmprint Database ⟨http://www.comp.polyu.edu.hk/~biometrics⟩.

[29] J. Daugman, The importance of being random: statistical principles of iris recognition, Pattern Recognition 36 (2003) 279–291.

[30] P.J. Phillips, H. Moon, S.A. Rizvi, P.J. Rauss, The FERET evaluation methodology for face-recognition algorithms, IEEE Transactions on Pattern Analysis and Machine Intelligence 22 (2000) 1090–1104.

[31] A. Jain, L. Hong, R. Bolle, On-line fingerprint verification, IEEE Transactions on Pattern Analysis and Machine Intelligence 19 (1997) 302–314.

[32] R. Snelick, U. Uludag, A. Mink, M. Indovina, A. Jain, Large-scale evaluation of multimodal biometric authentication using state-of-the-art systems, IEEE Transactions on Pattern Analysis and Machine Intelligence 27 (2005) 450–455.

[33] CASIA Palmprint Image Database V1.0 ⟨http://www.cbsr.ia.ac.cn⟩.

[34] D. Tao, X. Li, X. Wu, S.J. Maybank, General tensor discriminant analysis and Gabor features for gait recognition, IEEE Transactions on Pattern Analysis and Machine Intelligence 29 (2007) 1700–1715.

[35] D. Tao, X. Li, X. Wu, W. Hu, S.J. Maybank, Supervised tensor learning, Knowledge and Information Systems 13 (2007) 1–42.

[36] D. Tao, X. Li, X. Wu, S.J. Maybank, Geometric mean for subspace selection, IEEE Transactions on Pattern Analysis and Machine Intelligence 31 (2009) 260–274.

Wangmeng Zuo currently is a lecturer from School of Computer Science and Technology, Harbin Institute of Technology, Harbin, China. He received the Ph.D. degree in Computer Science and Technology from the Harbin Institute of Technology in 2007. He is a reviewer of several international journals, including IEEE Trans. Information Forensics and Security, IEEE Trans. Instrumentation and Measurement, IET Signal Processing, Neurocomputing, and International Journal of Image and Graphics. He is the author of 20 scientific papers in pattern recognition and computer vision. His current research interests include pattern recognition, computer vision, and their applications in biometrics, medical diagnosis, and bioinformatics.
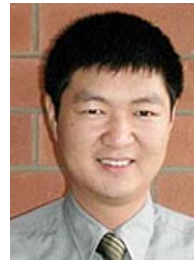
Lei Zhang received the B.S. degree in 1995 from Shenyang Institute of Aeronautical Engineering, Shenyang, PR China, the M.S. and Ph.D. degrees in Control Theory and Applications from Northwestern Polytechnical University, Xi'an, PR China, respectively in 1998 and 2001. From 2001 to 2002, he was a research associate in the Department of Computing, The Hong Kong Polytechnic University. From January 2003 to January 2006 he worked as a postdoctoral fellow in the Department of Electrical and Computer Engineering, McMaster University, Canada. Since January 2006, he has been an assistant professor in the Department of Computing, The Hong Kong Polytechnic University. His research interests include image and video processing, biometrics, pattern recognition, multisensor data fusion and optimal estimation theory, etc.

David Zhang (F'09) graduated in Computer Science from Peking University. He received his M.Sc. in Computer Science in 1982 and his Ph.D. in 1985 from the Harbin Institute of Technology (HIT). From 1986 to 1988 he was a Postdoctoral Fellow at Tsinghua University and then an Associate Professor at the Academia Sinica, Beijing. In 1994, he received his second Ph.D. in Electrical and Computer Engineering from the University of Waterloo, Ontario, Canada. Currently, he is a Head, Department of Computing, and a Chair Professor at the Hong Kong Polytechnic University where he is the Founding Director of the Biometrics Technology Centre (UGC/CRC) supported by the Hong Kong SAR Government in 1998. He also serves as Visiting Chair Professor in Tsinghua University, and Adjunct Professor in Peking University, Shanghai Jiao Tong University, HIT, and the University of Waterloo. He is the Founder and Editor-in-Chief, International Journal of Image and Graphics (IJIG); Book Editor, Springer International Series on Biometrics (KISB); Organizer, the International Conference on Biometrics Authentication (ICBA); Associate Editor of more than ten international journals including IEEE Transactions and Pattern Recognition; and the author of more than 10 books and 200 journal papers. Professor Zhang is a Croucher Senior Research Fellow, Distinguished Speaker of the IEEE Computer Society, and a Fellow of both IEEE and IAPR.

Zhenhua Guo received the B.S. and M.S. degree in Computer Science from Harbin Institute of Technology in 2002 and 2004, respectively. From 2005 to 2007, he was a research assistant with the Department of Computing, the Hong Kong Polytechnic University. Since August 2007, he has been a Ph.D. candidate at Department of Computing, the Hong Kong Polytechnic University. His research interests include pattern recognition, texture classification, biometrics, etc.